

Los Alamos National Laboratory is operated by the University of California for the United States Department of Energy under contract W-7405-ENG-36.

RECEIVED BY [unclear] JUL 07 1986

TITLE: FIBER OPTIC, FARADAY ROTATION CURRENT SENSOR

LA-UR--86-2084

DE86 012413

AUTHOR(S): L. R. Veeser, P-14
G. W. Day, NBS

SUBMITTED TO: Fourth International Conference on Megagauss Magnetic
Field Generation and Related Topics
Hilton Inn
Santa Fe, New Mexico

July 14-17, 1986

MASTER

By acceptance of this article, the publisher recognizes that the U.S. Government retains a nonexclusive, royalty-free license to publish or reproduce
the published form of this contribution, or to allow others to do so, for U.S. Government purposes

The Los Alamos National Laboratory requests that the publisher identify this article as work performed under the auspices of the U.S. Department of Energy

Los Alamos Los Alamos National Laboratory
Los Alamos, New Mexico 87545

FIBER OPTIC, FARADAY ROTATION CURRENT SENSOR

Lynn Veeser
Los Alamos National Laboratory, Los Alamos, NM

Gordon Day
National Bureau of Standards, Boulder, CO

INTRODUCTION

At the Second Megagauss Conference in 1979, there were reports of experiments that used the Faraday magneto-optic effect in a glass rod to measure large electric current pulses or magnetic fields.^{1,2} Since then we have seen the development of single-mode optical fibers that can carry polarized light in a closed loop around a current load. A fiber optic Faraday rotation sensor will integrate the flux, instead of sampling it at a discrete point, to get a measurement independent of the current distribution.

Early Faraday rotation experiments using optical fibers to measure currents dealt with problems such as fiber birefringence and difficulties in launching light into the tiny fiber cores.³⁻⁵ We have built on those experiments, working to reduce the effects of shocks and obtaining higher bandwidths, absolute calibration, and computerized recording and data analysis, to develop the Faraday rotation sensors into a routine current diagnostic. For large current pulses we find reduced sensitivity to electromagnetic interference and other backgrounds than for Rogowski loops; often the fiber optic sensors are useful where conductive probes cannot be used at all.

In this paper we describe the fiber optic sensors and some practical matters involved in fielding them.

SENSOR DESCRIPTION

Figure 1 shows a schematic of a typical sensor. Polarized 633-nm-wavelength light from a HeNe laser is focused into a single-mode fiber which encircles a current load some distance away and returns to the optics table in a shielded room. Light emerging from the fiber, with its polarization direction rotated by the current, is analyzed by a pair of Wollaston prisms separated by a partially reflecting mirror and rotated by 45° with respect to each other. A half wave retardation plate after the laser allows us to align the polarization in the fiber to minimize the effects of the fiber birefringence, and a similar plate after the fiber

rotates the polarization so that for zero current it is along the axis of one prism analyzer to simplify the data analysis. Detectors behind the prisms measure one or both of the polarization components.

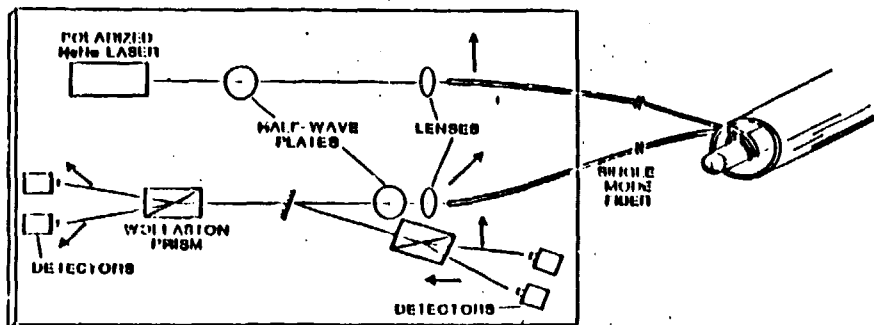


Fig. 1. Schematic of the polarimetric Faraday rotation sensor used at Los Alamos.

Instead of the HeNe laser, we sometimes use a GaAlAs diode laser with a fiber connected to it. This arrangement permits us to fuse the laser directly to the optical fiber. When we use, in addition, an in-line fiber optic polarization analyzer, we have an all-fiber-optic system suitable for remote operation. Polarization control can be obtained using an in-line retardation system that twists the fiber to change its birefringence.⁶⁻⁸ Since the diode lasers operate between 810 and 850 nm, they have less sensitivity, an advantage only for very large, fast pulses where the recording bandwidth is marginal.

Another arrangement that we have used successfully is the Sagnac interferometer, more commonly used as a fiber optic gyroscope to measure rotation rates. Here a coupler splits the laser light so that half goes in each direction around the loop. Index-of-refraction changes caused by the Faraday effect produce an interference fringe shift when the light is recombined in the fiber optic coupler. Because no polarization controllers or analyzers are needed, the interferometer is easily made into an all fiber-optic system; we have found it possible to field a Sagnac interferometer for < \$800 in equipment costs (exclusive of the detector).

The detectors that recorded most of our data are amplified photodiodes. Bandwidths of 100 to 400 MHz (depending on the housing used) and gains of 10^4 are obtained using a 10^3 -gain transimpedance current amplifier followed by a 10X voltage amplifier.⁹

We record the signals using a dual-beam, 200-M-sample/s programmable digitizer operated by an on-line computer. If we need faster response than the 5 ns sampling time can provide, we record in parallel on film. The computer stores the data on a disk for later analysis.

PRINCIPLES OF SENSOR OPERATION

The Faraday effect appears as a circular birefringence in the medium of the light propagation. That is, there is a difference between the

indices of refraction for beams of opposite circular polarization travelling in the glass fiber in the presence of a longitudinal magnetic field. This circular birefringence has the effect of rotating linearly polarized light by half the phase difference seen by circularly polarized beams.

The Faraday rotation angle θ can be found from

$$\theta = V' \int_0^L \vec{B} \cdot d\vec{x} ,$$

where V' is the Verdet constant for the material, \vec{B} is the magnetic field strength, and L is the path length in the field. Remembering Ampere's law for closed circuits,

$$I = \frac{1}{\mu_0} \int \vec{B} \cdot d\vec{x} ,$$

where I is the current crossing the surface bounded by the line integral, we see that $\theta = V' \mu_0 I N$ for a closed light path surrounding the current N times, independent of the path size and shape or the position of the current flow within it. We will refer to the quantity $V = V' \mu_0$ as the Verdet constant. In pure silica it is 4.62×10^{-6} rad/A or $264^\circ/MA$ for 633-nm-wavelength light, and it decreases with the square of the wavelength. Clearly, the Faraday effect is small enough that its most straightforward applications in pulsed current measurements are to large currents, although it is possible to increase the sensitivity, with some loss of bandwidth, by increasing the number of times the light circles around the current path, by changing the propagation material or the wavelength to increase the Verdet constant, or by measuring very small rotation angles.

The transmission of the light through the polarization analyzer depends on the relative orientations of the polarization and the analyzer. Two usual arrangements are to align the analyzer parallel to the direction of polarization for zero current or at 45° . In the first case, the transmission is proportional to $(1 + \cos 2\theta)$, and in the second case it varies as $(1 \pm \sin 2\theta)$. These two signals are shown as a function of current in Fig. 2. For small currents, the 45° alignment is more sensitive, but it can be difficult to achieve the exact orientation needed. When the current pulse is large enough to make the signal multi-valued ($\theta > \pi/4$), it can be difficult to determine the current from just one measured waveform unless more is known about the general shape. For large pulses it is often best to split the beam as shown in Fig. 1 and use two analyzers rotated by 45° with respect to each other. The resulting signals will be quadrature coded, i.e., 90° out of phase.

As with all other polarimetric fiber optic sensors, the performance of the Faraday rotation sensor depends on the polarization state of the light as it enters the sensor and as it evolves during the measurement. For an understanding of the sensor, it is especially important to understand the role played by birefringence in the fiber. Linear birefringence is a difference in the phase velocities of two orthogonally, linearly polarized beams having identical frequencies; circular birefringence is a similar difference for two beams of opposite circular polarization. When both effects are present, they combine in a complex manner that tends to favor

the larger one.¹⁰ Thus the Faraday effect (a circular birefringence change) can be almost completely obliterated by the presence of a large amount of linear birefringence, and smaller amounts can make the rotation angle a non-linear function of the magnetic field strength.

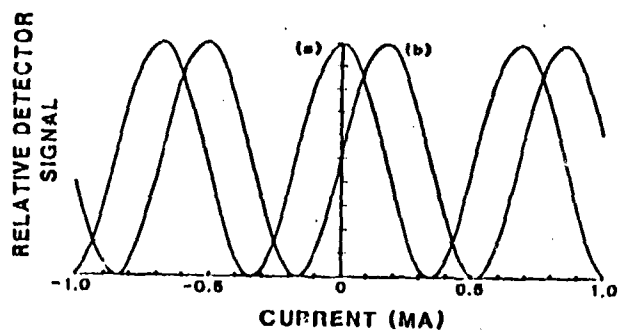


Fig. 2. Computed transfer functions for the sensor shown in Fig. 1 at a wavelength of 633 nm. a) Signal for polarizers aligned for maximum transmittance at zero current. b) Signal for analyzer rotated by 45° to give a transmittance of 0.5 at zero current.

Linear birefringence can arise from inherent geometrical imperfections or stress, or it may be induced by applied stress. It is possible to remove nearly all of the internal birefringence during manufacturing, for example, by spinning the preform while drawing the fiber.¹¹ Bending stress remains a problem, however. For silica fiber at a wavelength of 633 nm, an experimental value^{12,13} for the bend birefringence phase shift per unit length is $\delta_b = Kr^2/R^2$, where r is the fiber radius, R is the bend radius and $K = (7.6 \pm 0.05) \times 10^7$ deg/m. The bend birefringence varies approximately inversely with wavelength. Its effect on the transfer function of a sensor can be examined quantitatively.¹⁴ Calculated results for two cases are shown in Fig. 3a.

In any linearly and/or circularly birefringent medium there is a pair of orthogonal linear input polarization states for which the output polarization state is linear.¹⁵ For a fiber in which bend-induced birefringence is dominant, these axes are in and perpendicular to the plane of the bend. Light that enters the fiber linearly polarized along one of these axes remains linearly polarized. Consequently, this is the input condition that minimizes the effect of linear birefringence on the Faraday effect.

A good technique for overcoming induced linear birefringence is to twist the fiber.³ Twisting, like the Faraday effect, induces a rotation or circular birefringence in the fiber. The magnitude of the rotation is given by, $\Omega = g' \xi$, where Ω is the polarization rotation (half the circular birefringence), ξ is the twist, and g' is a material parameter which at a wavelength of 633 nm is^{16,17} about 0.07. The twist-induced rotation may be added algebraically to the magnetically-induced rotation. The effect on the transfer function is illustrated in Fig. 3b which shows that the benefit of twisting is, in essence, to bias the sensor away from the distorted part of the transfer function. The extent to which the transfer function can be shifted depends on the relative magnitudes of the linear birefringence and twist-induced rotation per turn and on the fiber strength. For a

given twist per unit length, the twist per turn increases linearly with coil diameter and bend-induced birefringence per turn varies inversely with the coil diameter; therefore, twisting becomes much more effective with larger coil diameters (Fig. 3b). For small coils it may not be possible to twist enough to measure dual polarity waveforms, but for monopolar electric pulses, less bias is required. We have been able to measure current pulses as small as 2A with a 10:1 signal-to-noise ratio for a 30 μ s pulse using a 100-turn, 10-cm-diam coil with the fiber twisted 15 twists/m.

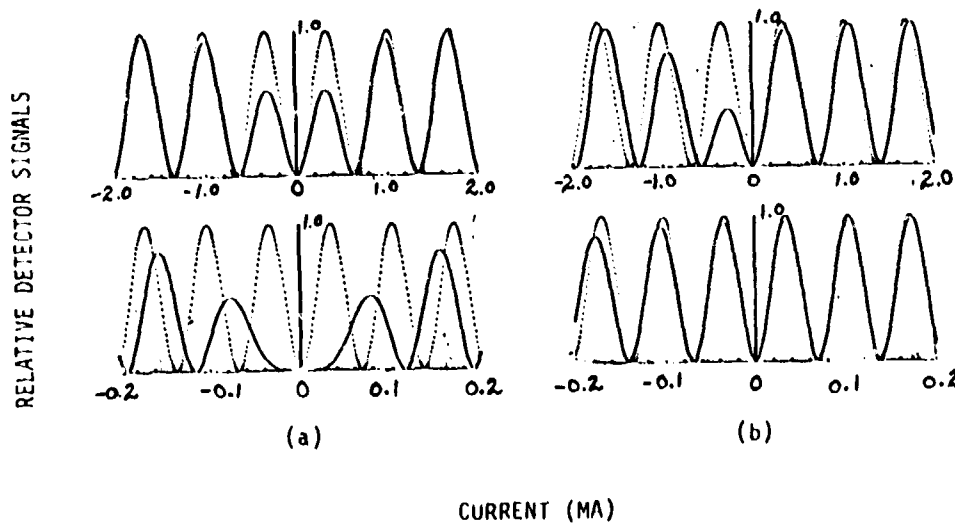


Fig. 3. Computed transfer functions of fiber current sensors showing (a) the effect of bend-induced linear birefringence in a 125 μ m-diam fiber operating at 633 nm wavelength, and (b) the effects of twisting the fiber. Upper curves are for a one-turn, 3-cm-diam fiber coil, lower curves are for a 10-turn, 10-cm-diam coil, and dotted curves assume no linear birefringence.

EXPERIMENT

Many of our sensor experiments have been fielded on capacitor bank shots for which the current pulse is a damped sine wave with a risetime (quarter cycle) of a few microseconds and a peak current of 1 to 5 MA. An example of raw data and a measured current pulse are shown in Fig. 4. Note the oscillations in the waveform near 0 and 12 μ s; they are smaller than the others because there was linear birefringence in the fiber and the polarization was not exactly aligned with it. When we have recorded data for longer times, we have seen the odd-shaped oscillations repeat every time the current reaches the value that produced it the first time, here slightly > 0 . On this shot the fiber was struck by a shock at 14 μ s, and the resulting birefringence destroyed the subsequent data. These data were taken using a double fiber loop of about 12 cm diameter, giving a Faraday rotation of 528°/MA; bending birefringence was estimated to be 70°, and the occurrence of the odd-shaped oscillations at a positive current rather than at zero indicates that some twist was likely present as well.

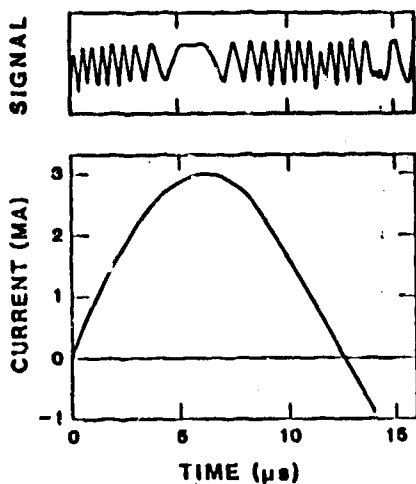


Fig. 4. Signal waveform (upper) and measured current (lower) for a 3 MA capacitor bank experiment. A 2-turn coil encircled the bank load. At 14 μ s a shock wave struck the fiber and obliterated the subsequent data.

Similar capacitor bank shots were used to develop high-current opening switches;^{18,19} we used the fiber optic sensors to measure the switched current because of their ability to fit easily into the tight geometry. In the coaxial systems,¹⁹ the fibers were looped with a diameter of 3 cm. We found it necessary to protect the fiber from shocks that struck it during the current flow, but even with protected fibers we sometimes experienced shock birefringence problems. Although we were able to get the needed data, we avoid such small fiber bends whenever possible.

Figure 5 shows a comparison between fiber optic sensors and carefully calibrated Rogowski loops for a two-stage, high-explosive-driven flux compression generator seeded by a bank. The output of the first stage was diagnosed with a HeNe laser system and the second stage was measured with a diode laser system, $\lambda = 808$ nm, for reduced sensitivity. The results are in agreement except that the second-stage fiber measured 3% more current than the Rogowski loop, apparently because the loop failed at high current. In general, the fibers and Rogowski loops agree to within $\pm 3\%$ on such shots; this is within their relative accuracies.

The largest uncertainty in calibrating the fiber optic sensors is the measurement of the Verdet constant. For bulk silica glass,²⁰⁻²² $V = 264^\circ/\text{MA} \pm 2\%$ at $\lambda = 632.8$ nm, and it decreases as the square of the wavelength. For silica doped with 3% GeO₂, typical of the fiber we used, we estimate that V increases by about 4% by assuming that $V \propto \lambda \frac{dn}{d\lambda}$ and using the dispersion values measured by Flemming.²³ For a doped-cladding fiber, estimating the change in V is difficult because the amount of light carried in the cladding varies from one fiber to another. For a fiber with a B₂O₃-doped cladding (Flemming does not give dispersions for fluorosilicate glasses) with 20% of the light in the cladding, we estimate a change in V of < 1%.

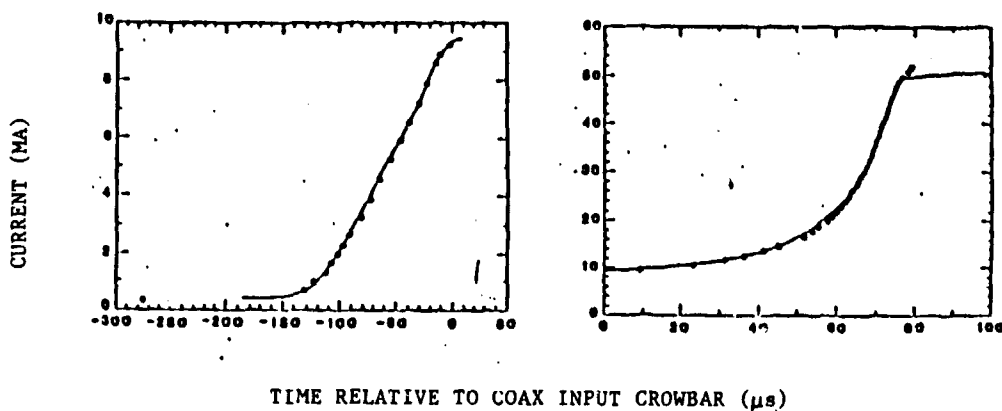


Fig. 6. Comparison of the fiber optic sensor (points) with a calibrated Rogowski loop (curves) for a 50 MA high-explosive-driven generator shot. The left graph shows the current measured at the output of the first stage of the flux compression generator, and the right one gives the current in the load after the second stage. The second Rogowski probe appears to have failed shortly before peak current, and consequently we do not have a comparison of the peak values measured.

To check our estimates of V for real fibers, we assembled the equipment necessary to measure it to high accuracy. For pure-silica-core fibers, the Verdet constant agreed with that of bulk glass to within $\pm 1.5\%$, while for doped-core fibers it varied from 0 to 3% higher.

We have begun to examine the Sagnac interferometer as a current sensor because, as an all-fiber device, it is especially adaptable to remote operation. Its response is the same as for a polarimetric Faraday rotation sensor with the polarization analyzers aligned, i.e., curve a of Fig. 2, but polarization control is not required because the sensor is an interferometer. We have collected Sagnac data from several experiments to prove the feasibility of the system and we are continuing to work to find a method to provide quadrature operation at high bandwidth to obtain linear sensitivity for small currents (curve b of Fig. 2).

REFERENCES

1. N. N. Gennadiev, V. F. Demichev, and P. A. Levit, "Production and measurement of megagauss magnetic fields in single-turn coils," in Megagauss Physics and Technology, P. J. Turchi, ed. (Plenum Press, NY and London, 1980), p. 27-36.
2. R. A. Nuttelman, J. H. Degnan, G. F. Kiutu, R. E. Reinovsky, and W. L. Baker, "Measurement of pulsed magnetic fields produced by flux compression in imploding liners," ibid., pp. 37-45.
3. S. C. Rashleigh and R. Ulrich, "Magneto-optic current sensing with birefringent fibers," Appl. Phys. Lett. 34, pp. 768-770 (1979).
4. A. M. Smith, "Optical fiber current measurement device at a generating station," Proc. SPIE 236, pp. 352-357 (1980).
5. E. H. Turner and R. H. Stolen, "Fiber Faraday circulator or isolator," Opt. Lett. 6, pp. 322-323 (1981).

6. H. C. Lefevre, "Single-mode fibre fractional wave devices and polarisation controllers," *Electron. Lett.* 16, pp. 778-780 (1980).
7. T. Okoshi, N. Fukaya, and K. Kikuchi, "New polarisation-state control device: rotatable fibre cranks," *Electron. Lett.* 21, pp. 895-896 (1985).
8. T. Matsumoto and H. Kano, "Endlessly rotatable fractional-wave devices for single-mode fibre optics," *Electron. Lett.* 22, pp. 78-79 (1986).
9. J. W. Ogle, R. C. Smith, M. Ward, R. Ramsey, and J. Hollabaugh, "A 100 MHz fiber optic single transient gamma-ray detection system," *Proc. SPIE 500*, pp. 134-140 (1984).
10. W. J. Tabor and F. S. Chen, "Electromagnetic Propagation through Materials Possessing both Faraday Rotation and Birefringence; Experiments with Ytterbium Orthoferrite," *J. Appl. Phys.* 40, pp. 2760-2765 (1969).
11. D. N. Payne, A. J. Barlow, and J. J. Ramskov Hansen, "Development of Low- and High-Birefringence Optical Fibers," *IEEE J. Quantum Electron.* 18, pp. 477-488 (1982).
12. R. Ulrich, S. C. Rashleigh, and W. Eickhoff, "Bending-induced birefringence in single-mode fibers," *Opt. Lett.* 5, pp. 273-275 (1980).
13. G. W. Day, D. N. Payne, A. J. Barlow, and J. J. Ramskov-Hansen, "Faraday rotation in coiled, monomode optical fibers; isolators, filters, and magnetic sensors," *Opt. Lett.* 7, pp. 238-240 (1982).
14. A. M. Smith, "Polarization and magneto-optic properties of single-mode optical fiber," *Appl. Opt.* 17, pp. 52-56 (1978).
15. A. Papp and H. Harms, "Polarization optics of index-gradient optical waveguide fibers," *Appl. Optics* 14, pp. 2406-2411 (1975).
16. R. Ulrich and A. Simon, "Polarization optics of twisted single-mode fibers," *Appl. Opt.* 18, pp. 2241-2251 (1979).
17. A. M. Smith, "Birefringence induced by bends and twists in single-mode optical fiber," *Appl. Opt.* 19, pp. 2606-2611 (1980).
18. D. R. Kania, L. A. Jones, E. L. Zimmermann, L. R. Veeser, and R. J. Trainor, "Experimental investigation of a magnetic gate as a multimegapere, vacuum opening switch," *Appl. Phys. Lett.* 44, pp. 741-743 (1984).
19. D. R. Kania, E. L. Zimmermann, R. J. Trainor, L. R. Veeser, and L. A. Jones, "Experimental tests of a moving foil as a high current vacuum opening switch," *Appl. Phys. Lett.* 45, pp. 26-28 (1984).
20. W. B. Garn, R. S. Caird, C. M. Fowler, and D. B. Thompson, "Measurement of Faraday Rotation in Megagauss Fields over the Continuous Visible Spectrum," *Rev. Sci. Instrum.* 39, pp. 1313-1317 (1968).
21. S. Ramaseshan, "Determination of the magneto-optic anomaly of some glasses," *Proc. Indian Acad. Sci.* 24, pp. 426-432 (1946).
22. N. George, R. W. Wanek, and S. W. Lee, "Faraday Effect at Optical Frequencies in Strong Magnetic Fields," *Appl. Opt.* 4, pp. 253-254 (1965).
23. J. W. Fleming, "Material and Mode Dispersion in $Ge_2\cdot B_2O_3\cdot SiO_2$ Glasses," *J. Am. Ceramic Soc.* 59, pp. 503-507 (1976).

DISCLAIMER

This report was prepared as an account of work sponsored by an agency of the United States Government. Neither the United States Government nor any agency thereof, nor any of their employees, makes any warranty, express or implied, or assumes any legal liability or responsibility for the accuracy, completeness, or usefulness of any information, apparatus, product, or process disclosed, or represents that its use would not infringe privately owned rights. Reference herein to any specific commercial product, process, or service by trade name, trademark, manufacturer, or otherwise does not necessarily constitute or imply its endorsement, recommendation, or favoring by the United States Government or any agency thereof. The views and opinions of authors expressed herein do not necessarily state or reflect those of the United States Government or any agency thereof.